Journal Pre-proofs

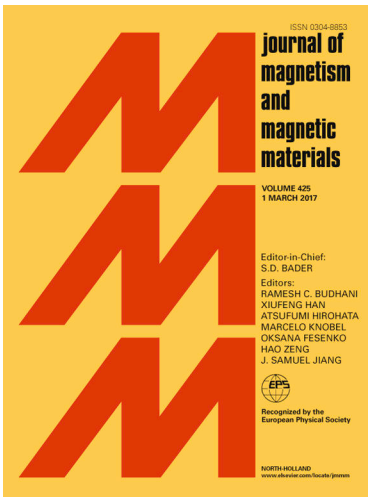

Research article

Hysteretic Magnetic Field Analysis with Second-Order Homogenization

Tetsuji Matsuo

PII: S0304-8853(24)00002-7
DOI: https://doi.org/10.1016/j.jmmm.2024.171713
Reference: MAGMA 171713

To appear in: *Journal of Magnetism and Magnetic Materials*

Received Date: 13 October 2023
Revised Date: 15 December 2023
Accepted Date: 1 January 2024

Please cite this article as: T. Matsuo, Hysteretic Magnetic Field Analysis with Second-Order Homogenization, *Journal of Magnetism and Magnetic Materials* (2024), doi: https://doi.org/10.1016/j.jmmm.2024.171713

Hysteretic Magnetic Field Analysis with Second-Order Homogenization

Tetsuji Matsuo[a,*]

[a]Graduate School of Engineering, Kyoto University, Kyoto, 615-8510, Kyoto, Japan

Abstract: A dynamic hysteresis model represented by the Cauer circuit was combined with the finite element analysis to efficiently compute magnetic field in micro-structured iron-cores. A finite element eddy-current analysis with higher order homogenization method is reformulated to implement the Cauer circuit representation. Three types of hysteretic Cauer circuits for the 2nd-order homogenization were examined. The analysis of wounded core under sinusoidal excitation showed that the 2nd order homogenization scheme with finite difference approximation improved the accuracy of representation of iron loss and current-flux loops. The 2nd-order scheme also improved the accuracy of homogenized representation under pulse-width-modulation excitation. The computation time was greatly reduced by the homogenization schemes.

Keywords: Cauer circuit, dynamic hysteresis, laminated core, second-order homogenization, play model.

1. Introduction

Many iron-core materials are microscopically insulated, such as powder and laminated cores, to reduce eddy-current loss. To design magnetic devices using these materials, the magnetic field analysis must be conducted to evaluate the eddy-current in the microstructure. However, the direct eddy-current analysis within the microstructure using the finite element (FE) method requires a very fine FE mesh, which is computationally expensive.

To avoid handling the microstructure directly, homogenization methods have been developed [1-4], which provide averaged magnetic properties to handle micro-structured materials as uniform solid materials. Refs. [2, 3] presented a FE formulation to implement the 2nd order homogenization scheme for representing laminated core, which enables us to handle micro-structured materials without using a microscopically fine mesh.

The Cauer circuit can efficiently and accurately represent the homogenized eddy-current field. It was proven equivalent to the homogenization method in Ref. [2] in the case of laminated core [5] with linear magnetic property. Following are benefits of the Cauer circuit representation: (i) it can be combined with a hysteresis model to represent a dynamic hysteretic property [5], (ii) it allows for a more general representation of micro-structured materials other than laminated cores [4], and (iii) higher-order homogenization scheme can be directly derived [6]. Because of the equivalence of Cauer circuit representation to the homogenization method, it is expected to be combined with the FE analysis.

The hysteretic Cauer circuit has several versions, which have not been formulated for the homogenized FE analysis, yet. This study generalizes the homogenized FE formulation for the laminated core to handle the Cauer circuit representation including the case of hysteretic circuit. It realizes an efficient magnetic field analysis of micro-structured cores using 2nd-order homogenization. A higher order formulation is also presented. Three versions of hysteretic Cauer circuit representations are compared in the analysis of wounded core.

2. Cauer Circuit Representation

The dynamic property of magnetic material is often represented effectively using the Cauer circuit [Fig. 1], where H and dB/dt are the input current and voltage, respectively. The circuit equations are given as

$$H = \frac{\varphi_0}{L_0} + G_1\left(\frac{\mathrm{d}\varphi_0}{\mathrm{d}t} - \frac{\mathrm{d}\varphi_2}{\mathrm{d}t}\right), \tag{1}$$

$$0 = \frac{\varphi_{2n}}{L_{2n}} - G_{2n-1}\frac{\mathrm{d}\varphi_{2n-2}}{\mathrm{d}t} + (G_{2n-1} + G_{2n+1})\frac{\mathrm{d}\varphi_{2n}}{\mathrm{d}t} - G_{2n+1}\frac{\mathrm{d}\varphi_{2n+2}}{\mathrm{d}t} \quad (n = 1, 2, \ldots), \tag{2}$$

where L_{2n} and G_{2n+1} are the inductance and conductance, respectively, and φ_{2n} is the magnetic flux of L_{2n}. In many cases, L_{2n} and G_{2n+1} (n = 1, 2, ...) are smaller than L_0 and G_1 to represent the magnetic property in a higher frequency range. For convenience of nonlinearization, the c_{2n} (ratio of inductance) is defined as

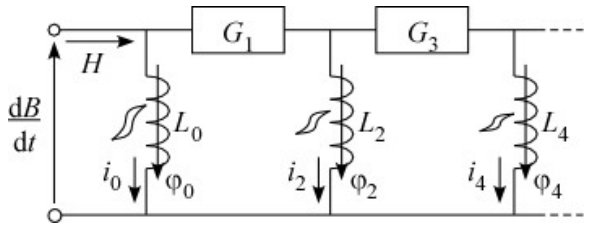

Figure 1: Cauer circuit representation

$$L_{2n} = \frac{L_0}{c_{2n}}. \tag{3}$$

Using c_{2n}, φ_{2n} is transformed as

$$\varphi_{2n} = \frac{B_{2n}}{c_{2n}}. \tag{4}$$

The circuit equations are rewritten as

$$H = \frac{B_0}{c_0 L_0} + g_0\frac{\mathrm{d}B_0}{\mathrm{d}t} - g_1\frac{\mathrm{d}B_2}{\mathrm{d}t}, \tag{5}$$

$$0 = \frac{B_{2n}}{c_{2n}L_0} - g_{2n-1}\frac{\mathrm{d}B_{2n-2}}{\mathrm{d}t} + g_{2n}\frac{\mathrm{d}B_{2n}}{\mathrm{d}t} - g_{2n+1}\frac{\mathrm{d}B_{2n+2}}{\mathrm{d}t} \quad (n = 1, 2, \ldots) \tag{6}$$

where g_{2n} and g_{2n+1} are given with $G_{-1} = 0$ as

$$g_{2n} = \frac{G_{2n-1} + G_{2n+1}}{c_{2n}^2}, \; g_{2n+1} = \frac{G_{2n+1}}{c_{2n}c_{2n+2}}. \tag{7}$$

The first inductor L_0 represents the static magnetic property h_{dc} as

$$\frac{\varphi_0}{L_0} = \frac{B_0}{L_0} = h_{\mathrm{dc}}(B_0)\,, \tag{8}$$

where h_{dc} is the static magnetic field. The property of L_{2n} at latter ladder stages is represented as

$$\frac{\varphi_{2n}}{L_{2n}} = \frac{B_{2n}}{L_0} = h(B_{2n})\,. \tag{9}$$

When h_{dc} is a single-valued function of B_0 and current i_0 is dominant, $h(B_{2n})$ can be given by the differential permeability [5] as

$$h(B_{2n}) = \frac{B_{2n}}{\mu_{\mathrm{d}}}\,, \tag{10}$$

where

$$\frac{1}{\mu_{\mathrm{d}}} = \frac{\mathrm{d}h_{\mathrm{dc}}(B_0)}{\mathrm{d}B_0}\,. \tag{11}$$

However, when h_{dc} is a hysteretic function, a simple formula (10) is not valid. Ref. [5] proposed several methods for obtaining $h(B_{2n})$ as follows.

(i) the simple approximation:

$$h(B_{2n}) = h_{\mathrm{dc}}(B_{2n})\,. \tag{12}$$

(ii) the finite difference approximation:

$$h(B_{2n}) = \frac{h_{\mathrm{dc}}(B_0 + \varepsilon B_{2n}) - h_{\mathrm{dc}}(B_0)}{\varepsilon}\,, \tag{13}$$

where ε is a constant. Eq. (13) is a similar version to (10) in the presence of hysteretic property.

(iii) the reversible approximation

$$h(B_{2n}) = \nu_{\mathrm{rev}}(B_{2n})\,, \tag{14}$$

where

$$\nu_{\mathrm{rev}} = \frac{\mathrm{d}h_{\mathrm{rev}}(B_0)}{\mathrm{d}B_0}\,, \tag{15}$$

where $h_{\mathrm{rev}}(B_0)$ is the reversible component of $h_{\mathrm{dc}}(B_0)$. The reversible approximation is effective when the higher harmonic components yield small minor loops as in the case of pulse-width-modulation (PWM) excitation [5].

The Cauer circuit representation is extended to the dynamic vector hysteretic property as:

$$\boldsymbol{H} = \boldsymbol{h}_{\mathrm{dc}}(\boldsymbol{B}_0) + g_0 \frac{\mathrm{d}\boldsymbol{B}_0}{\mathrm{d}t} - g_1 \frac{\mathrm{d}\boldsymbol{B}_2}{\mathrm{d}t}\,, \tag{16}$$

$$0 = \frac{\boldsymbol{h}(\boldsymbol{B}_{2n})}{c_{2n}} - g_{2n-1}\frac{\mathrm{d}\boldsymbol{B}_{2n-2}}{\mathrm{d}t} + g_{2n}\frac{\mathrm{d}\boldsymbol{B}_{2n}}{\mathrm{d}t} - g_{2n+1}\frac{\mathrm{d}\boldsymbol{B}_{2n+2}}{\mathrm{d}t} \quad (n = 1, 2, ...) . \tag{17}$$

Homogenized representations of core material are given by truncating the Cauer circuit.

The 0th order homogenization is given as

$$\boldsymbol{H} = \boldsymbol{h}_{\mathrm{dc}}(\boldsymbol{B}_0) + g_0\frac{\mathrm{d}\boldsymbol{B}_0}{\mathrm{d}t}, \tag{18}$$

which corresponds to the classical eddy-current theory [7].

The 2nd order homogenization is given as

$$\begin{aligned} \boldsymbol{H} &= \boldsymbol{h}_{\mathrm{dc}}(\boldsymbol{B}_0) + g_0\frac{\mathrm{d}\boldsymbol{B}_0}{\mathrm{d}t} - g_1\frac{\mathrm{d}\boldsymbol{B}_2}{\mathrm{d}t}, \\ 0 &= \frac{\boldsymbol{h}(\boldsymbol{B}_2)}{c_2} - g_1\frac{\mathrm{d}\boldsymbol{B}_0}{\mathrm{d}t} + g_2\frac{\mathrm{d}\boldsymbol{B}_2}{\mathrm{d}t} . \end{aligned} \tag{19}$$

In the case of laminated core, c_2, g_0, g_1 and g_2 are given as

$$c_2 = 5 , \; g_0 = \frac{\sigma d^2}{12} , \; g_1 = \frac{\sigma d^2}{60} , \; g_2 = \frac{\sigma d^2}{210} \tag{20}$$

where σ is the electric conductivity and d is the sheet thickness [2, 5].

Both representations (18) and (19) can be implemented in the FE analysis through the homogenization procedure proposed in previous studies [2, 3].

3. Homogenized Hysteretic Magnetic Field Analysis

The Cauer circuit representation is combined with the magnetic field analysis. For simplicity, 2-dimensional magnetic field with the vector potential $\boldsymbol{A} = (0, 0, A)$ is discussed in this paper.

When the 0th order homogenization (18) is used, the magnetic field equation is written as

$$\mathrm{curl}[\boldsymbol{h}_{\mathrm{dc}}(\boldsymbol{B}) + g_0\mathrm{curl}\frac{\partial \boldsymbol{A}}{\partial t}] = -\sigma\frac{\partial \boldsymbol{A}}{\partial t} + \boldsymbol{J}_{\mathrm{S}} , \tag{21}$$

where $\boldsymbol{J}_{\mathrm{S}} = (0, 0, J_{\mathrm{S}})$ is the source current density,

$$\boldsymbol{h}_{\mathrm{dc}}(\boldsymbol{B}) = (h_{\mathrm{dcx}}(\boldsymbol{B}), h_{\mathrm{dcy}}(\boldsymbol{B}), 0) , \tag{22}$$

$$\boldsymbol{B} = (B_x, B_y, 0) = (\frac{\partial A}{\partial y}, -\frac{\partial A}{\partial x}, 0) , \tag{23}$$

and σ is the conductivity of the materials that are not homogenized. For simplicity, the term $-\sigma\partial\boldsymbol{A}/\partial t$ is omitted hereafter.

When the 2nd order homogenization (19) is used, the magnetic field equation becomes

$$\mathrm{curl}[\boldsymbol{h}_{\mathrm{dc}}(\boldsymbol{B}_0)+g_0\mathrm{curl}\frac{\partial \boldsymbol{A}_0}{\partial t}-g_1\mathrm{curl}\frac{\partial \boldsymbol{A}_2}{\partial t}]=\boldsymbol{J}_{\mathrm{S}}$$

$$\mathrm{curl}[\frac{\boldsymbol{h}(\boldsymbol{B}_2)}{c_2}-g_1\mathrm{curl}\frac{\partial \boldsymbol{A}_0}{\partial t}+g_2\mathrm{curl}\frac{\partial \boldsymbol{A}_2}{\partial t}]=0 \tag{24}$$

$$\boldsymbol{A}_0=(0,0,A_0)\ ,\ \boldsymbol{A}_2=(0,0,A_2) \tag{25}$$

$$\boldsymbol{h}(\boldsymbol{B})=(h_x(\boldsymbol{B}),h_y(\boldsymbol{B}),0) \tag{26}$$

$$\boldsymbol{B}_0=(\frac{\partial A_0}{\partial y},-\frac{\partial A_0}{\partial x},0),\ \ \boldsymbol{B}_2=(\frac{\partial A_2}{\partial y},-\frac{\partial A_2}{\partial x},0)\,. \tag{27}$$

A weak form for FE analysis involving 2nd order homogenization is given as

$$F_0(A_0,A_2)=0\ ,\ F_2(A_0,A_2)=0\,, \tag{28}$$

where

$$\begin{aligned}F_0(A_0,A_2)=\int_\Omega[&-h_{\mathrm{dcy}}(\boldsymbol{B}_0)\frac{\partial w_0}{\partial x}+h_{\mathrm{dcx}}(\boldsymbol{B}_0)\frac{\partial w_0}{\partial y}+g_0\frac{\mathrm{d}}{\mathrm{d}t}(\frac{\partial A_0}{\partial x}\frac{\partial w_0}{\partial x}+\frac{\partial A_0}{\partial y}\frac{\partial w_0}{\partial y})\\&-g_1\frac{\mathrm{d}}{\mathrm{d}t}(\frac{\partial A_2}{\partial x}\frac{\partial w_0}{\partial x}+\frac{\partial A_2}{\partial y}\frac{\partial w_0}{\partial y})-J_{\mathrm{S}}w_0]\mathrm{d}\Omega\end{aligned} \tag{29}$$

$$\begin{aligned}F_2(A_0,A_2)=\int_\Omega[&-\frac{h_y(\boldsymbol{B}_2)}{c_2}\frac{\partial w_2}{\partial x}+\frac{h_x(\boldsymbol{B}_2)}{c_2}\frac{\partial w_2}{\partial y}-g_1\frac{\mathrm{d}}{\mathrm{d}t}(\frac{\partial A_0}{\partial x}\frac{\partial w_2}{\partial x}+\frac{\partial A_0}{\partial y}\frac{\partial w_2}{\partial y})\\&+g_2\frac{\mathrm{d}}{\mathrm{d}t}(\frac{\partial A_2}{\partial x}\frac{\partial w_2}{\partial x}+\frac{\partial A_2}{\partial y}\frac{\partial w_2}{\partial y})]\mathrm{d}\Omega\end{aligned}\,. \tag{30}$$

Here, w_0 and w_2 are weighting functions for the FE analysis.

In the 2N-th order case, a weak form is given as

$$F_{2n}(A_{2n-2},A_{2n},A_{2n+2})=0\ (n=1,...,N-1)\,, \tag{31}$$

where

$$\begin{aligned}F_{2n}(A_{2n-2},A_{2n},A_{2n+2})=\int_\Omega[&-\frac{h_y(\boldsymbol{B}_{2n})}{c_{2n}}\frac{\partial w_{2n}}{\partial x}+\frac{h_x(\boldsymbol{B}_{2n})}{c_{2n}}\frac{\partial w_{2n}}{\partial y}-g_{2n-1}\frac{\mathrm{d}}{\mathrm{d}t}(\frac{\partial A_{2n-2}}{\partial x}\frac{\partial w_{2n}}{\partial x}+\frac{\partial A_{2n-2}}{\partial y}\frac{\partial w_{2n}}{\partial y})\\&+g_{2n}\frac{\mathrm{d}}{\mathrm{d}t}(\frac{\partial A_{2n}}{\partial x}\frac{\partial w_{2n}}{\partial x}+\frac{\partial A_{2n}}{\partial y}\frac{\partial w_{2n}}{\partial y})-g_{2n+1}\frac{\mathrm{d}}{\mathrm{d}t}(\frac{\partial A_{2n+2}}{\partial x}\frac{\partial w_{2n}}{\partial x}+\frac{\partial A_{2n+2}}{\partial y}\frac{\partial w_{2n}}{\partial y})]\mathrm{d}\Omega\end{aligned}\,. \tag{32}$$

For n = 0, Eq. (32) is replaced by (29). For n = N, terms with respect to A_{2n+2} are omitted.

4. Computational Results

4.1. Simulation with Sinusoidal Input

A laminated core with 20 wound sheets [Fig. 2(a)] was analyzed. Owing to the insulation coating, the homogenized laminated core has an anisotropic property, which is mentioned in Appendix. The static hysteretic property is represented by the isotropic vector play model [8]. The hysteretic property shown in Fig. 2(b) was used in the analysis. The conductivity of core material is 2×10^6 S/m.

Figure 3 shows the iron losses simulated with 0th and 2nd order homogenizations, which were compared with the loss given by the FE analysis with fine mesh ("fem"); the excitation frequency f was 200, 1 k, and 4 kHz with the coil voltage of $0.03f$ and $0.06f$ V. The backward Euler scheme was used for the time integration with the time-step of $1/60f$. Three types of 2nd order schemes were compared: the simple approximation (12) ("simp"), the finite difference approximation (13) ("dif") with $\varepsilon = 0.5$, and the reversible approximation (14) ("rev"). All the homogenization schemes gave accurate loss when f is small. In the case of low amplitude, 0th order scheme and 2nd order scheme with reversible approximation overestimated the loss as higher than 1 kHz. The 2nd-order scheme with simple approximation underestimated the loss at high frequency range. Figure 4 shows the current-flux loops simulated with 0th and 2nd order schemes. When the frequency was low, all the homogenization schemes yielded accurate loops. The 0th order scheme and 2nd order scheme with reversible approximation failed to reconstruct accurate current-flux loops at 4 kHz. Figure 5 shows the average discrepancy of current given by the homogenization schemes compared with the FE analysis with fine mesh. The 2nd order scheme with finite difference approximation obtained relatively accurate current-flux loops.

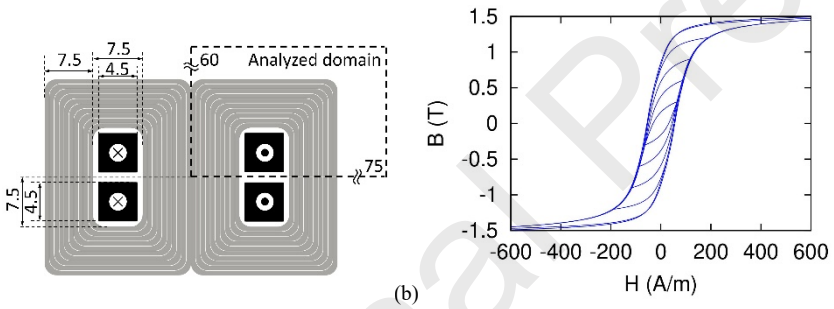

Figure 2: Analysis of wounded core: (a) core shape and (b) hysteretic property of core material

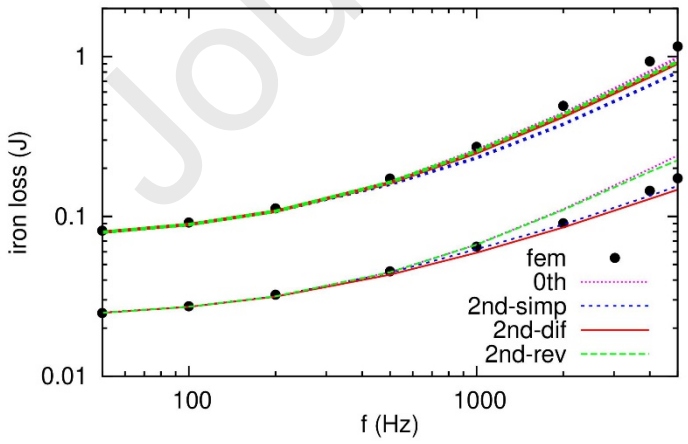

Figure 3: Iron loss per cycle

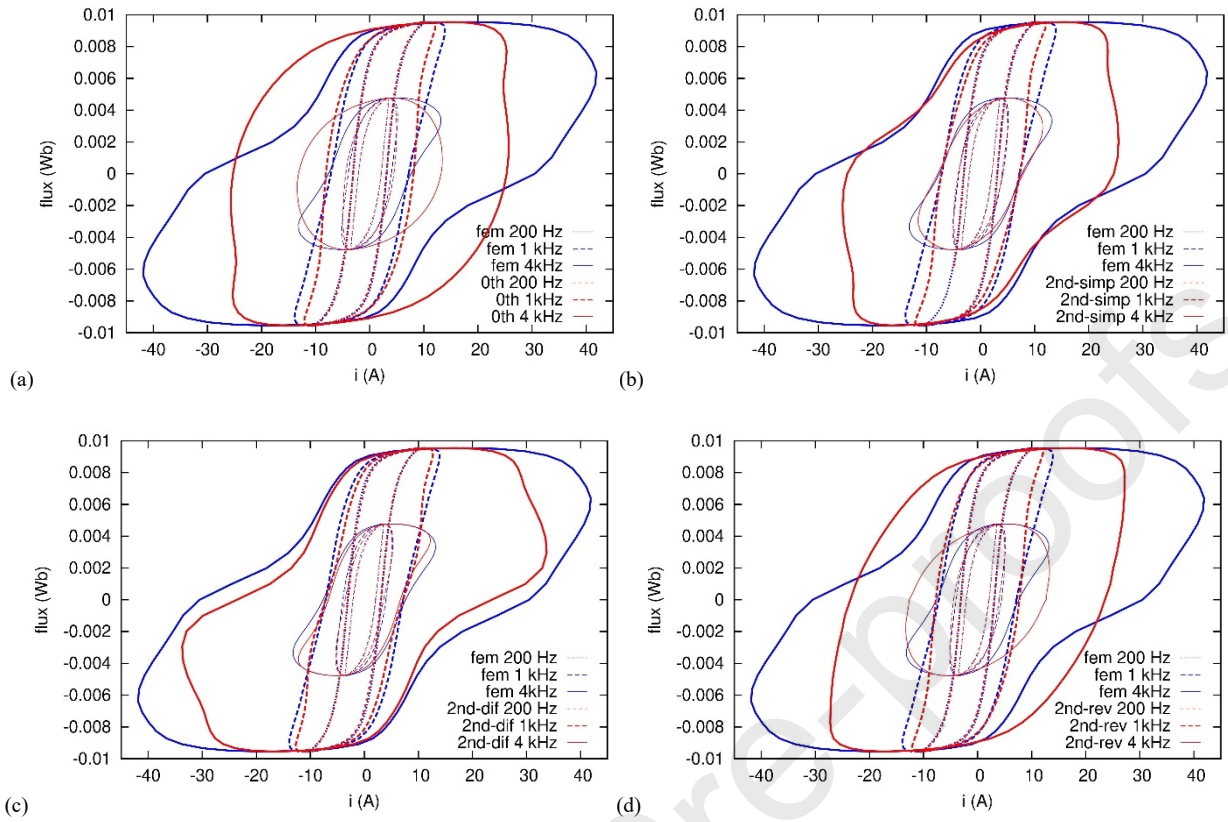

Figure 4: Simulated current-flux loops: (a) 0th order homogenization, and 2nd order homogenizations with (b) simple, (c) finite difference, and (d) reversible approximations.

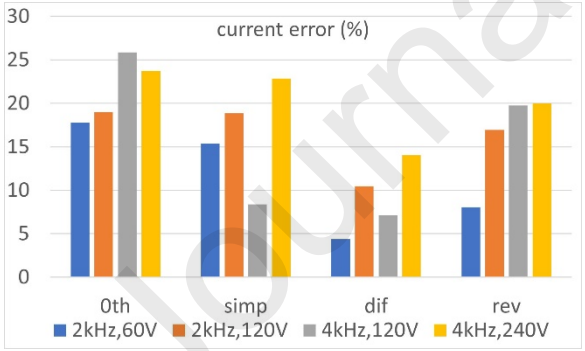

Figure 5: Discrepancy of current compared with FE analysis with fine mesh.

A free software FreeFEM++ was used to execute the abovementioned computations using a desktop PC. The FE analysis without homogenization needs finer computational grid for higher frequency, which requires 170 and 712 min for 1-period analysis at 1 and 4 kHz, respectively. The homogenized schemes do not need a finer grid, which require 7.1, 15.4, 16.5, and 13.7 min using the 0th order scheme and 2nd order schemes with the simple, finite difference, and reversible approximations, respectively. The homogenization schemes effectively reduced the computational cost.

4.2. Simulation with PWM Input

Figure 6 shows the simulated current-flux curves under PWM excitation with the modulation of 0.5 given by the FE analyses with fine mesh and the 0th- and 2nd-order homogenizations. The fundamental and carrier frequencies were 50 and 3750 Hz, respectively. The time step was 1/1500f. The term $g_0 \mathrm{d}\boldsymbol{B}_0/\mathrm{d}t$ of 0th order scheme directly reflected the pulsive voltage waveform, whereas the 2nd order schemes improved the representation of minor hysteresis loops rounded by the inductive effect. The FE analysis required 8.2 days, whereas the homogenized schemes required 1.7, 2.1, and 4.5 hours using the 0th order scheme and 2nd order scheme with the finite difference and reversible approximations, respectively.

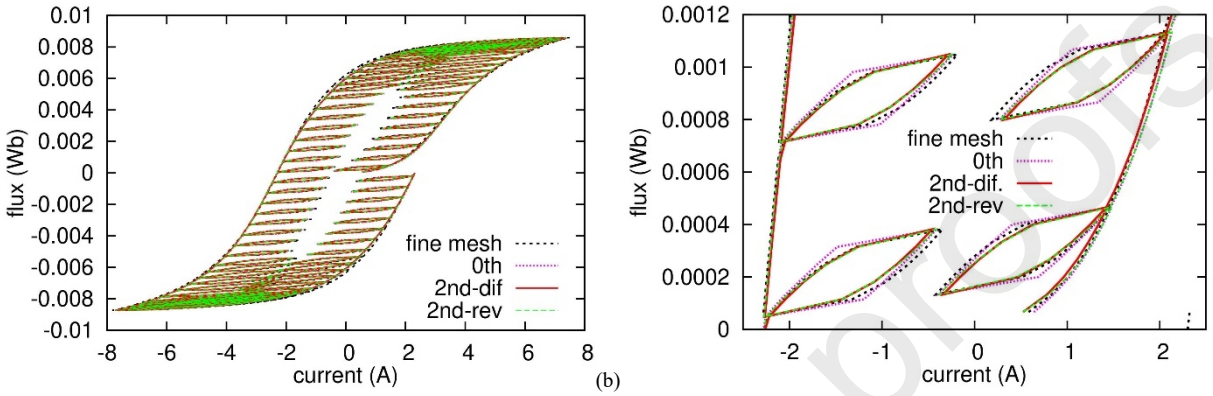

Figure 6: Simulated current-flux curves: (a) for one time period and (b) enlarged view.

5. Concluding Remarks

The 2nd-order homogenized magnetic field analysis was reformulated to implement a hysteretic Cauer circuit representation, where a micro-structured iron-core was used as a solid material. The hysteretic Cauer circuit representations with the simple, the finite difference, and the reversible approximations were examined. The analysis of wounded core under sinusoidal excitation showed that all the homogenization schemes yielded accurate iron loss and current-flux property when the frequency is low. The 0th order scheme and 2nd order scheme with reversible approximation overestimated the iron loss when the amplitude is small and the frequency is high. whereas the 2nd-order scheme with simple approximation underestimated the loss at high frequency range. The 0th order scheme and 2nd order scheme with simple and reversible approximations failed to reconstruct accurate current-flux loops when the frequency is high whereas the 2nd order scheme with finite difference approximation obtained relatively accurate magnetic properties. The 2nd-order scheme also improved the accuracy of homogenized representation of the laminated core under PWM excitation. The computation time was greatly reduced by the homogenization schemes. The proposed method will be a powerful tool for computer aided design of magnetic devices.

Acknowledgment

This work was supported in part by the MEXT-Program for Creation of Innovative Core Technology for Power Electronics, Grant Number JPJ009777.

References

[1] O. Bottauscio, M. Chiampi, D. Chiarabaglio, "Advanced model of laminated magnetic cores for two-dimensional field analysis," IEEE Trans. Magn., vol. 36, pp. 561–573, May 2000.

[2] J. Gyselinck, P. Dular, “A time-domain homogenization technique for laminated iron cores in 3-D finite-element models,” IEEE Trans. Magn., vol. 40, pp. 856–859, Mar. 2004.

[3] J. Gyselinck, R.V. Sabariego, P. Dular, “A nonlinear time-domain homogenization technique for laminated iron cores in three-dimensional finite-element models,” IEEE Trans. Magn., vol. 42, pp. 763–766, Apr. 2006.

[4] S. Hiruma, H. Igarashi, "Homogenization method based on Cauer circuit via unit cell approach," IEEE Trans. Magn., vol. 56, 7505805, 2020.

[5] Y. Shindo, T. Miyazaki, T. Matsuo. "Cauer circuit representation of the homogenized eddy-current field based on the Legendre expansion for a magnetic sheet," IEEE Trans. Magn., vol. 52, 6300504, 2016.

[6] H. Eskandari, J. Gyselinck, T. Matsuo, Nonlinear multi-scale model order reduction of eddy-current problems, IEEE Trans. Magn. vol. 58, 6300305, 2022.

[7] G. Bertotti, Hysteresis in Magnetism, Academic Press, 1998.

[8] R. Mitsuoka, T. Mifune, T. Matsuo, C. Kaido, "A vector play model for finite-element magnetic-field analysis with Newton-Raphson method," IEEE Trans. Magn., vol. 49, pp. 1689–1692, 2013.

Appendix

In the case of steel sheet, the homogenized equations (18) and (19) give the in-plane property of the steel. The tangential and normal components $\boldsymbol{B}$ and $\boldsymbol{H}$ of the sheet are denoted as (B_t, B_n) and (H_t, H_n), respectively. The magnetic flux in the tangential direction is dominated by the flux in the steel, whereas the reluctivity in the normal direction is dominated by the reluctivity of the insulation. Hence, the anisotropic property is written as

$$H_\mathrm{t} \approx h_\mathrm{st}\left(\frac{B_\mathrm{t}}{\alpha}, B_\mathrm{n}\right)\ ,\ H_\mathrm{n} \approx (1-\alpha)\frac{B_\mathrm{n}}{\mu_0}, \tag{33}$$

where α is the fill factor, B_t/α is the magnetic flux density in the steel, h_st represents the magnetic property in the steel given by $\boldsymbol{h}_\mathrm{dc}$ or $\boldsymbol{h}$ in (18) and (19), and μ_0 is the permeability of the insulator.

The FE analysis handles the macroscopic field (B_x, B_y), from which (H_x, H_y) are calculated as follows. From (B_x, B_y), (B_t, B_n) can be calculated as

$$B_\mathrm{t} = B_x\cos\theta + B_y\sin\theta\ ,\ B_\mathrm{n} = -B_x\sin\theta + B_y\cos\theta, \tag{34}$$

where θ is the angle of tangential direction. After obtaining (H_t, H_n) using (33), (H_x, H_y) are obtained as

$$H_x = H_\mathrm{t}\cos\theta - H_\mathrm{n}\sin\theta,\ H_y = H_\mathrm{t}\sin\theta + H_\mathrm{n}\cos\theta, \tag{35}$$

which are returned to the FE analysis.

- A dynamic hysteresis model represented by the Cauer circuit was combined with the finite element analysis to efficiently compute magnetic field in micro-structured iron-cores.
- A finite element formulation with a higher order homogenization method is presented for hysteretic eddy-current analysis.
- The 2nd-order scheme successfully improved the accuracy of the homogenized representation of laminated core under sinusoidal and PWM excitations.